agriculture

MDPI

Article

Spatial Drivers of the Electricity-to-Water Conversion Coefficient in an Inner Mongolia Plateau Irrigation District

Hao Zhang [1,2,3,†], Bowen Gao [1,4,†], Xiaohong Shi [1,2,*], Junping Lu [1,2,3], Yu Liu [1,2], Wei Li [3] and Longmei Xie [1]

[1] State Key Laboratory of Water Engineering Ecology and Environment in Arid and Semi-Arid Regions, Inner Mongolia Agricultural University, Hohhot 010018, China; nndzhanghao@163.com (H.Z.); nmgnydxgbw@163.com (B.G.); junping516@163.com (J.L.); yuliu@imau.edu.cn (Y.L.); nndsjy2024@163.com (L.X.)
[2] College of Water Resources and Civil Engineering, Inner Mongolia Agricultural University, Hohhot 010018, China
[3] Inner Mongolia Autonomous Region Environmental Science Society, Hohhot 010018, China; nmghjkxxh2021@163.com
[4] College of Desert Control Science and Engineering, Inner Mongolia Agricultural University, Hohhot 010018, China
* Correspondence: imaushixiaohong@163.com
† These authors contributed equally to this work and should be considered co-first authors.

Abstract

Groundwater accounting in arid and semi-arid well-irrigated areas is often constrained by difficulties in water-meter installation and maintenance, as well as variability in well–pump operation, thereby limiting refined agricultural water-use management. The electricity-to-water conversion coefficient (Tc) can be used to estimate groundwater abstraction from electricity consumption; however, the applicability of empirical models developed for plain irrigation districts remains uncertain in plateau regions characterized by pronounced topographic relief and complex aquifer conditions. This study examined 56 typical irrigation wells in Chayouzhongqi on the Inner Mongolia Plateau. Based on pumping-test data and using correlation analysis, structural equation modeling, redundancy analysis, and random forest analysis, we investigated the spatial distribution of Tc and its associated mechanisms. Tc ranged from 0.08 to 3.88 m^3 kWh^{-1}, with a mean of 1.62 m^3 kWh^{-1}, and exhibited a pattern of higher values in the north, lower values in the south, and the lowest values in the western part of the study area. Electricity consumption, rated flow rate, and actual discharge were the principal associated variables, with relative importance values of 43.0%, 21.6%, and 15.7%, respectively. Topographic and aquifer conditions imposed regional constraints on spatial variation in Tc by influencing well–pump operating states. These findings indicate that Tc estimation in plateau well-irrigation districts should not directly adopt empirical relationships developed for plains, but should instead be calibrated according to regional hydrogeological and engineering operating conditions, thereby providing a basis for improved groundwater accounting and water-saving management in arid and semi-arid regions.

Keywords: water–energy nexus; pump operation; groundwater accounting; hydrogeological heterogeneity; regional calibration

Check for updates

Academic Editor: Gerard Arbat

Received: 20 May 2026
Revised: 28 June 2026
Accepted: 30 June 2026
Published: 2 July 2026

Copyright: © 2026 by the authors. Licensee MDPI, Basel, Switzerland. This article is an open access article distributed under the terms and conditions of the Creative Commons Attribution (CC BY) license.

1. Introduction

Water scarcity and the transition toward low-carbon energy systems are dual challenges for sustainable agriculture worldwide. These challenges are particularly acute in arid

and semi-arid regions, where irrigation commonly relies on groundwater abstraction and the water–energy nexus is especially pronounced [1–3]. The electricity-to-water conversion coefficient (Tc) links irrigation electricity consumption with groundwater withdrawal and therefore provides a practical basis for electricity-based water accounting in pumping-well irrigation systems [4]. Tc reflects the operational performance of well–pump systems and may also be associated with geological setting, aquifer water-yield potential, groundwater depth, pumping head, pump characteristics, and irrigation practices. Its spatial and temporal variability can directly affect the accuracy of groundwater accounting and the effectiveness of coordinated water- and energy-management measures [5–7].

Previous studies in China have mainly examined Tc in relatively flat irrigation districts in North China and Northeast China. These studies have often relied on single factors or a limited set of variables and have focused on statistical relationships between Tc, groundwater levels, and water withdrawal [8,9]. Although such work provides a useful basis for electricity-based groundwater accounting, the transferability of empirical relationships across regions remains uncertain. Compared with plain irrigation districts, plateau irrigation areas are characterized by pronounced topographic relief, heterogeneous aquifer conditions, and substantial variation in groundwater depth and pumping head. These conditions may affect individual-well yield, pumping conditions, and well–pump operating states, thereby indirectly influencing Tc. Consequently, empirical coefficients developed for plains should not be directly transferred to plateau irrigation districts without regional assessment and calibration.

Chayouzhongqi is located in the central part of the Inner Mongolia Plateau, where agricultural irrigation is highly dependent on groundwater abstraction. The study area includes substantial variation in well depth, pump power, irrigation methods, topographic setting, and aquifer conditions, providing a representative setting for comparing typical well–pump systems under contrasting operating and hydrogeological conditions [10–14].

Accordingly, this study investigated 56 typical irrigation wells in Chayouzhongqi to (1) characterize the spatial variation in Tc across the plateau irrigation district; (2) distinguish direct well–pump operating variables from external hydrogeological and topographic constraints; and (3) develop an in-sample regional calibration equation for Tc under the observed conditions. To avoid interpreting definitional dependence as independent causality, electricity consumption (E) and actual discharge (Q) were treated as direct operational variables because both enter the calculation of Tc, whereas rated flow rate (Qr) was considered an indicator of pump configuration and operating capacity. Variables including elevation, well depth, groundwater depth, aquifer water-yield potential, and lithology were treated as external hydrogeological or topographic constraints. We tested the following hypotheses:

(1) Tc exhibits spatial heterogeneity in plateau irrigation districts, and its distribution is constrained by topographic and aquifer conditions.
(2) Within-sample variation in Tc is primarily represented by differences in electricity consumption, actual discharge, and rated flow rate as direct well–pump operating variables.
(3) A regional calibration based on key well–pump operating variables, interpreted within the local hydrogeological setting, can describe within-sample Tc variation and provide a basis for location-specific groundwater accounting.

2. Materials and Methods

2.1. Study Area

Chayouzhongqi (41°16′–43°30′ N, 114°45′–115°05′ E) is located in the central part of Ulanqab City, Inner Mongolia Autonomous Region, China. It has a total area of 4190 km^2 [10] and is characterized by a temperate continental climate [11], with a mean

annual precipitation of 322.7 mm and evaporation of up to 1500 mm [12]. Water resources are scarce and unevenly distributed in time and space. The landscape is dominated by hills, plains, and river valleys [12], and the main groundwater types include fractured-porous groundwater and porous groundwater [13]. As an agriculture-dominated region [14], Chayouzhongqi has an annual agricultural irrigation water use of approximately 58 million m^3, of which agricultural water use accounts for more than 90%. Agricultural irrigation is highly dependent on groundwater abstraction, whereas water-use efficiency remains relatively low and energy consumption is high [11]. Chayouzhongqi contains 4758 motor-pumped wells across 12 townships. Among the 56 selected typical wells, 49 were equipped for drip irrigation, five for sprinkler irrigation, and two for pipe irrigation. Five wells were selected in Bayin Township, four in Datang Township, twelve in Guangyilong Town, seven in Hongpan Township, five in Huangyangcheng Town, four in Kobol Town, two in Kulun Sumu, six in Tieshagai Town, five in Tuchengzi Township, two in Ulan Sumu, and four in Wusuotu Town. The six irrigation wells in Huitengxile Industrial Park lacked individual electricity meters; because electricity-use and water-discharge data could not be obtained simultaneously, they were not included in the typical-well monitoring network [11,13].

2.2. Data Sources

This study followed a typical well approach to infer regional conditions from representative cases. Well selection considered the topography, hydrogeological conditions, distribution characteristics of well-irrigated areas, and well–pump operating types in Chayouzhongqi, with reference to hydrogeological survey results from the previous studies and regional hydrogeological data [15]. In July 2023, 56 typical monitoring wells were selected using a stratified sampling approach (Figure 1). During testing at each monitoring well, continuous single-well observations were conducted for no less than 24 h until water-level variation approached stability, defined as a change in less than 0.02 m over three consecutive hours. A high-precision pressure-type water-level logger (accuracy: ±0.01 m) with automatic recording and data-storage capabilities was used to continuously obtain high-temporal-resolution water-level data, thereby ensuring the stability and comparability of the observations. These 56 wells were not selected through complete random sampling from all 4758 motor-pumped wells in Chayouzhongqi; rather, they were selected to cover the principal spatial differences and well–pump operating types within the study area.

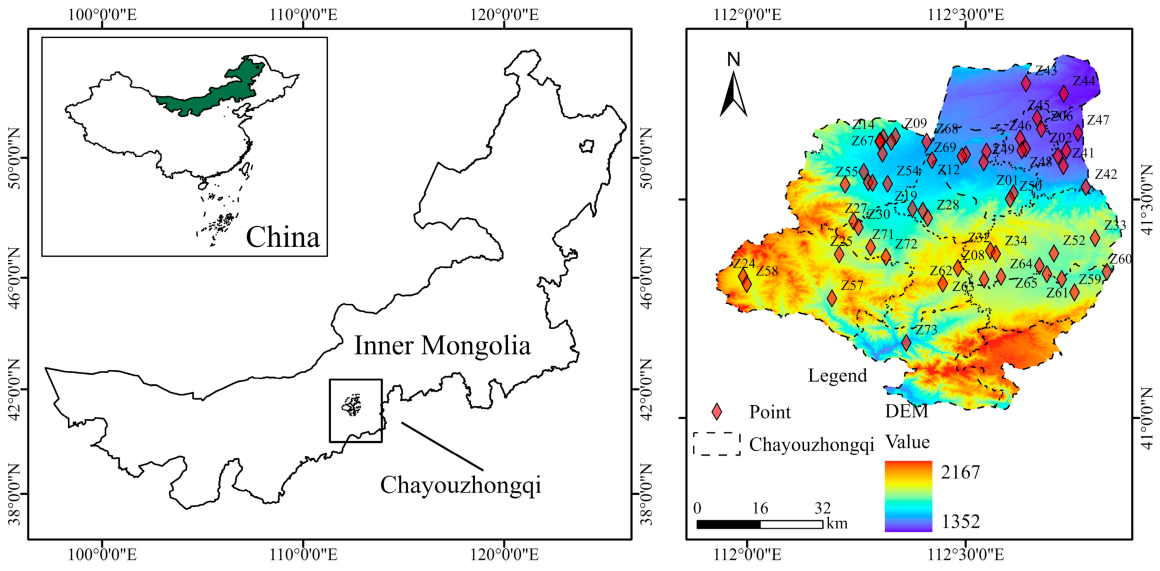

Figure 1. Sampling point location.

The selection of typical wells considered the following criteria: (1) landform type, including the northern plains, southern hills, and western mountainous areas; (2) well depth, including 0–50 m, 50–100 m, 100–150 m, 150–200 m, and >200 m; (3) pump power and rated flow rate, representing low-, medium-, and high-capacity operating types; (4) irrigation method, including drip irrigation, sprinkler irrigation, and pipe irrigation; and (5) the availability of electricity-meter and water-discharge data that could be read synchronously. Some wells in Huitengxile Industrial Park lacked individual electricity meters; therefore, simultaneous electricity-use and water-discharge data could not be obtained. These wells were not included in the typical-well monitoring network.

The field survey included the electricity-to-water conversion coefficient (Tc), actual discharge (Q), electricity consumption (E), elevation (H), aquifer water-yield potential (W), well depth (D), groundwater depth (GD), lithology (LT), rated flow rate (Qr), pump power (P), well completion date (T), casing inside diameter (R), and irrigated area (S). Actual discharge and electricity consumption were obtained through synchronized readings from flow meters and electricity meters during normal irrigation operation, and Tc was calculated accordingly [16]. Elevation was obtained using GPS measurements [17]. Well depth, well completion date, and casing inside diameter were obtained from construction records or well-completion archives. Groundwater depth was measured using an electric contact water-level meter [18]. Lithology was identified based on regional geological exploration reports and drilling records [11]. Rated flow rate and pump power were obtained from equipment nameplates, whereas irrigated area was determined through field surveys and irrigation-district planning data.

Aquifer water-yield potential and lithology were primarily determined using regional hydrogeological data, geological investigation reports, and drilling records [13]. Because lithology is a categorical variable, it cannot be directly included in correlation analysis, redundancy analysis (RDA), structural equation modeling (SEM), or random forest analysis. Therefore, lithology was assigned ordinal scores according to its hydrogeological implications. Lithologies with low permeability and low water-yield capacity were assigned lower values; lithologies with intermediate permeability or water-yield capacity were assigned intermediate values; and lithologies with high permeability and strong water-yield capacity were assigned higher values. This treatment was intended to reflect the potential constraints imposed by different lithological conditions on well discharge capacity and the electricity-to-water conversion process. It should be noted that this assignment is a semi-quantitative treatment based on hydrogeological significance and is intended primarily to compare relative differences in Tc among lithological conditions; it does not represent precise physical parameters of the lithologies themselves.

Raw data were organized, checked, and summarized using Excel 2024. Origin 2024 was used to generate trend plots and correlation plots. SPSS 28 was used for regression analysis, correlation analysis, and significance testing. Amos 21.0 was used to construct the structural equation model of factors associated with Tc, and ArcGIS 10.8 was used to produce spatial distribution maps [19]. Definitions of all abbreviated variables are provided in figure captions and table notes to improve the readability of figures and tables.

2.3. Analysis Methods

2.3.1. Electricity-to-Water Conversion Coefficient

Electricity consumption was measured using electricity meters, whereas water discharge was measured using flow meters [7,20]. The electricity-to-water conversion coefficient was calculated from the proportional relationship between electricity consumption and water discharge as follows:

$$T_c = \frac{W}{E} = \frac{QT}{E} \quad (1)$$

where *Tc* is the electricity-to-water conversion coefficient (m^3 kWh^{-1}); *W* is the total volume of water discharged during the measurement period *T* (m^3); *Q* is the water discharge rate during *T* (m^3h^{-1}); *T* is the duration of the measurement period; and *E* is the electricity consumption during *T* (kWh). It should be noted that *Q* and *E* are direct components of the *Tc* calculation. They were therefore treated as well–pump operating-state variables rather than simply interpreted as independent external environmental factors.

The arithmetic mean ($\overline{x}$) assigns equal weight to all observations and was calculated as follows:

$$\overline{x} = \frac{x_1 + x_2 + x_3 + \ldots + x_n}{n} \quad (2)$$

where x_i is the *Tc* value of the *i*-th typical well, and *n* is the number of typical wells [21].

2.3.2. Correlation Analysis

Pearson correlation analysis was used to preliminarily identify relationships between Tc and well–pump operating variables and hydrogeological variables. The variables included in the analysis were Q, E, H, W, D, GD, LT, Qr, P, T, R, and S. Continuous variables were directly included in the correlation analysis. Categorical variables, including lithology (LT), were assigned ordinal values according to their hydrogeological significance before being included in the analysis. The significance level was set at $p < 0.05$. Pearson's correlation coefficient was calculated as follows:

$$r = \frac{\sum (x_i - \overline{x})(y_i - \overline{y})}{\sqrt{\sum (x_i - \overline{x})^2 (y_i - \overline{y})^2}} \quad (3)$$

where *r* is Pearson's correlation coefficient; x_i and y_i are the *i*-th observations of variables *x* and *y*, respectively; and $\overline{x}$ and $\overline{y}$ are the mean values of variables x and y, respectively. The correlation coefficient ranges from -1 to 1 [22].

2.3.3. Structural Equation Modeling

Structural equation modeling (SEM) was used to further examine the path relationships between well–pump operating variables and hydrogeological variables and to establish a framework describing the relationships between Tc and the main associated variables. The model was specified based on the correlation analysis and hydrogeological understanding, with particular attention to direct and indirect relationships among Tc, Q, E, Qr, GD, LT, W, P, and S [21,22]. An SEM model generally comprises a measurement model and a structural model. The measurement model was expressed as follows:

$$\Upsilon = A_y \eta + \epsilon \quad (4)$$

where Υ is the vector of observed variables; *Ay* is the loading matrix between observed variables and latent variables; η is the vector of latent variables; and ϵ is the error term.

The structural model was expressed as follows:

$$\Theta = \Gamma\Theta + BX + \zeta \quad (5)$$

where Θ is the vector of latent variables; Γ is the matrix describing relationships among latent variables; *B* is the matrix describing relationships between latent variables and exogenous variables; *X* is the vector of exogenous observed variables; and ζ is the error term. SEM results were used to describe statistical path relationships and possible directions of association among variables and were not interpreted as strict causal evidence.

2.3.4. Redundancy Analysis

Redundancy analysis (RDA) was used to evaluate the overall explanatory capacity of well–pump operating variables and hydrogeological variables for variation in *Tc*, *Q*, and *E*. Variables with different units were standardized before analysis to reduce the influence of differences in measurement scales. The explanatory variables included H, W, D, GD, LT, Qr, P, T, R, and S, whereas the direct effects of actual discharge (Q) and electricity consumption (E) on Tc were excluded. RDA was used to identify the overall directions of association between these variables and *Tc*, *Q*, and *E*, and the results were interpreted together with the correlation analysis and random forest results [21,22]. The calculation was expressed as follows:

$$Y = X\beta + \epsilon \tag{6}$$

where Y is the response-variable matrix, X is the explanatory-variable matrix, β is the regression coefficient, and ϵ is the error term.

2.3.5. Random Forest Model

A random forest regression model was used to evaluate the relative importance of different variables for *Tc*, with actual discharge (*Q*) and electricity consumption (*E*) excluded to avoid their direct mathematical effects on Tc. Because Tc is a continuous variable, mean squared error (MSE) was used as the splitting criterion at each node. The reduction in MSE attributable to each variable across all decision trees was used as the variable-importance metric. MSE was calculated as follows:

$$MSE = \frac{1}{n}\sum_{i=1}^{n}\left(y_i - \widetilde{y_i}\right)^2 \tag{7}$$

where y_i is the observed value, $\widetilde{y_i}$ is the predicted value, and n is the number of observations in a node. During node splitting, the reduction in MSE (ΔMSE) attributable to a variable was used to evaluate its contribution to the model.

Based on the reduction in MSE attributable to each variable across all decision trees, the importance of variable *j*, *VIj*, was defined as follows:

$$VI_j = \frac{\sum_{t=1}^{T}\sum_{S\epsilon S_j}\Delta MSE_{s,t}}{\sum_{j=1}^{p}\sum_{t=1}^{T}\sum_{S\epsilon S_j}\Delta MSE_{s,t}} \tag{8}$$

where T is the number of trees in the random forest; S_j is the set of nodes split using variable *j*; Δ*MSEs*, *t* is the reduction in MSE before and after splitting node s in tree *t*; and p is the total number of input variables. A larger *VI* value indicates greater relative importance of the variable and can be used to identify variables more strongly associated with within-sample variation in *Tc* [21,22]. The stability of the random forest model was internally evaluated using a training–testing split, cross-validation, and out-of-bag error.

3. Results

3.1. Spatial Distribution of the Electricity-to-Water Conversion Coefficient

In Chayouzhongqi, Tc ranged from 0.08 to 3.88 m^3 kWh^{-1}, with an arithmetic mean of 1.62 m^3 kWh^{-1}. This means that, on average, 1.62 m^3 of groundwater can be extracted per kilowatt-hour of electricity in the study area. Spatially, Tc exhibited a north-to-south decreasing pattern, with the lowest values occurring in the western part of the study area (Figure 2). The maximum Tc value was 3.88 m^3 kWh^{-1} and occurred at well Z11 in Tieshagai Town and well Z55 in Guangyilong Town. The minimum value was 0.08 m^3 kWh^{-1} and occurred at well Z57 in Datang Township (Table 1).

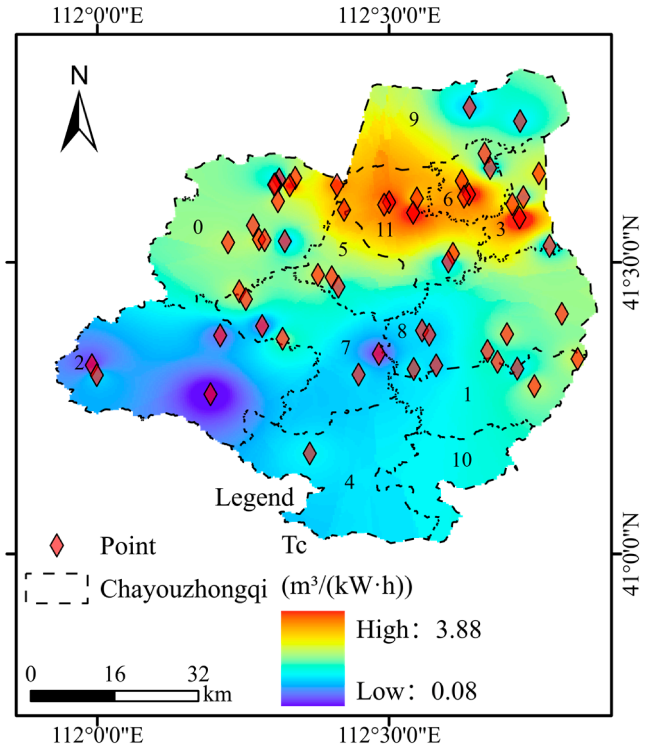

Figure 2. Spatial distribution of the electricity-to-water conversion coefficient in Chayouzhongqi. Note: 0 represents Guangyilong Town, 1 represents Kobol Town, 2 represents Datian Township, 3 represents Wusutu Town, 4 represents Ulan Sumu, 5 represents Tuchengzi Township, 6 represents Bayin Township, 7 represents Huangyangcheng Town, 8 represents Hongpan Township, 9 represents Kuytun Sum, 10 represents Huitengxile Industrial Park, and 11 represents Tieshagai Town.

Table 1. Electricity-to-water conversion coefficients by township in Chayouzhongqi.

No.	Township	Monitoring Well	Electricity-to-Water Conversion Coefficient (m^3/(kW·h))	Range	Mean ± Standard Deviation
1	Wusutu Town	Z47	1.68	1.06~2.45	1.58 ± 0.56
2		Z04	1.11		
3		Z42	2.45		
4		Z41	1.06		
5		Z02	1.6		
6	Ulan Sum	Z73	1.63	0.41~1.63	1.02 ± 0.86
7		Z62	0.41		
8	Tuchengzi Township	Z70	0.6	0.6~3.35	1.59 ± 1.21
9		Z28	0.78		
10		Z19	0.88		
11		Z29	3.35		
12		Z69	2.36		
13	Tieshagai Town	Z12	2.63	0.98~3.88	1.98 ± 1.13
14		Z13	1.12		
15		Z01	1.97		
16		Z50	1.26		
17		Z11	3.88		
18		Z49	0.98		
19	Kulun Sum	Z44	3.25	2~3.25	2.63 ± 0.88
20		Z43	2		

Table 1. *Cont.*

No.	Township	Monitoring Well	Electricity-to-Water Conversion Coefficient (m^3/(kW·h))	Range	Mean ± Standard Deviation
21	Kobul Town	Z59	1.5	1.5~1.83	1.66 ± 0.14
22		Z63	1.83		
23		Z61	1.61		
24		Z60	1.68		
25	Huangyangcheng Town	Z27	1.84	1.07~2.15	1.75 ± 0.41
26		Z72	2.15		
27		Z30	1.07		
28		Z08	1.7		
29		Z71	1.97		
30	Hongpan Township	Z34	1.77	1.11~2.22	1.67 ± 0.47
31		Z32	1.39		
32		Z65	2.21		
33		Z52	1.84		
34		Z64	1.14		
35		Z51	2.22		
36		Z33	1.11		
37	Guangyilong Town	Z15	1.59	0.31~3.88	1.64 ± 1.09
38		Z14	1.04		
39		Z66	1.81		
40		Z67	3.25		
41		Z09	0.46		
42		Z17	1.84		
43		Z16	1.76		
44		Z56	1.15		
45		Z68	0.31		
46		Z55	3.88		
47		Z54	0.98		
48	Datang Township	Z24	1.93	0.08~1.93	0.91 ± 0.78
49		Z58	1.01		
50		Z25	0.61		
51		Z57	0.08		
52	Bayin Township	Z45	1.25	0.91~1.83	1.41 ± 0.38
53		Z06	0.91		
54		Z48	1.75		
55		Z74	1.3		
56		Z46	1.83		

3.2. Relationships Between the Electricity-to-Water Conversion Coefficient and Associated Variables

Pearson correlation analysis was used to examine the relationships between Tc and actual discharge, electricity consumption, elevation, aquifer water-yield potential, well depth, groundwater depth, rated flow rate, pump power, well completion date, casing inside diameter, and irrigated area in Chayouzhongqi (n = 56; Figures 3 and 4). Linear fitting showed that Tc was significantly and positively correlated with rated flow rate ($p < 0.001$, $R^2 = 0.62$) and actual discharge ($p < 0.001$, $R^2 = 0.62$), whereas it was negatively correlated with electricity consumption ($p < 0.01$, $R^2 = 0.41$).

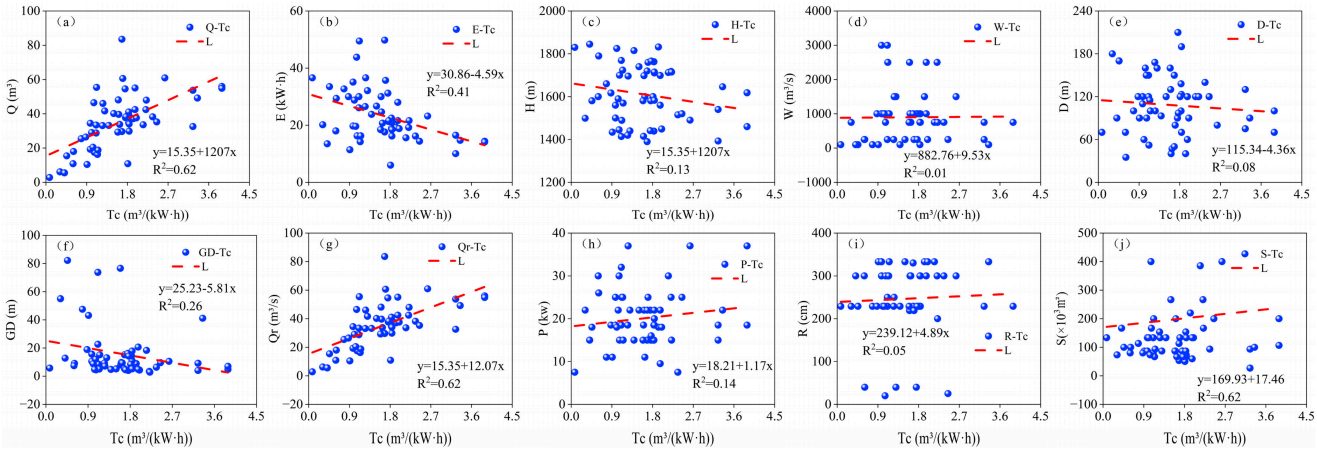

Figure 3. Linear fits between the electricity-to-water conversion coefficient (Tc) and associated variables. (**a**) Actual discharge (Q); (**b**) Electricity consumption (E); (**c**) Elevation (H); (**d**) Aquifer water-yield potential (W); (**e**) Well depth (D); (**f**) Groundwater depth (GD); (**g**) Rated flow rate (Qr); (**h**) Pump power (P); (**i**) Casing inside diameter (R); (**j**) Irrigated area (S). Note: L denotes the fitted line.

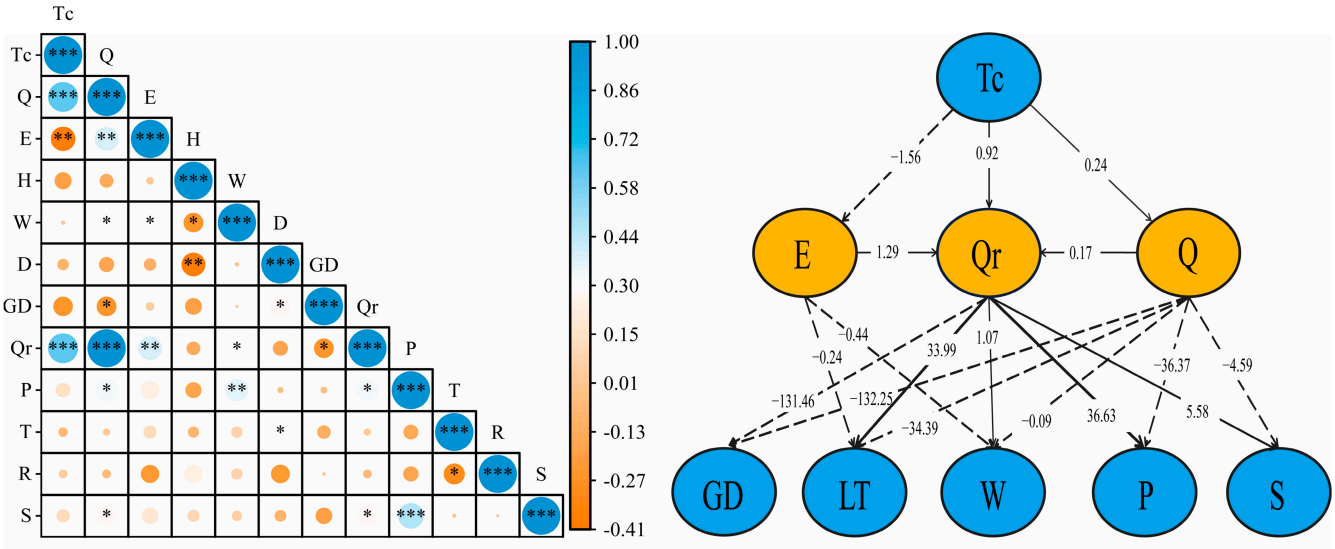

Figure 4. Correlation matrix between the electricity-to-water conversion coefficient and associated variables (**left**) and structural equation model (SEM) diagram (**right**). Note: * $p \leq 0.05$, ** $p \leq 0.01$, and *** $p \leq 0.001$. Lithology (LT) is a categorical variable. Because permeability and water-yield capacity differ substantially among lithological conditions, lithology was assigned ordinal scores according to its hydrogeological significance. Lithologies with low permeability were assigned lower values, whereas lithologies with high permeability were assigned higher values, to reflect the potential influence of lithological conditions on well discharge capacity and the electricity-to-water conversion coefficient.

3.3. Structural Characteristics of the Electricity-to-Water Conversion Coefficient and Influencing Factors

Based on the correlation-analysis framework described above, a structural equation model was constructed to examine the relationships between Tc and associated variables in Chayouzhongqi (Figure 4 and Table 2). Because electricity consumption and actual discharge directly enter the calculation of Tc, the paths involving Tc, electricity consumption, and actual discharge primarily reflect statistical associations among variables and well–pump operating-state relationships; they were not interpreted as strict causal effects.

Table 2. SEM path coefficients.

Path	Unstandardized Coefficient	Standardized Coefficient	Standard Error	Z	*p*
Electricity-to-water conversion coefficient → Actual discharge	4.123	0.242	0.794	5.19	0.000 ***
Rated flow rate → Actual discharge	0.689	0.689	0.035	19.966	0.000 ***
Electricity-to-water conversion coefficient → Electricity consumption	−13.529	−1.561	2.216	−6.105	0.000 ***
Actual discharge → Pump power	−11.971	−36.37	154.615	−0.077	0.938
Rated flow rate → Pump power	12.057	36.633	154.61	0.078	0.938
Actual discharge → Irrigation area	−9.518	−4.585	5.208	−1.827	0.068 *
Rated flow rate → Irrigation area	11.592	5.584	5.208	2.226	0.026 **
Actual discharge → Aquifer water-yield potential	−1.203	−0.087	2.081	−0.578	0.563
Electricity consumption → Aquifer water-yield potential	−12.011	−0.44	7.641	−1.572	0.116
Rated flow rate → Aquifer water-yield potential	14.879	1.074	2.082	7.148	0.000 ***
Actual discharge → Groundwater depth	−54.86	−132.246	33.061	−1.659	0.097 *
Rated flow rate → Groundwater depth	54.53	131.455	33.058	1.65	0.099 *
Actual discharge → Lithology	−1.584	−34.386	15.887	−0.1	0.921
Electricity consumption → Lithology	−0.022	−0.241	0.014	−1.537	0.124
Rated flow rate → Lithology	1.566	33.985	15.887	0.099	0.921

Note: Only estimable paths for which complete standard errors, Z values, and *p*-values were obtained are presented. *** indicates $p < 0.001$ and ** indicates $p < 0.05$. * Results with $0.05 \leq p < 0.10$ are described only as marginal associations.

The SEM regression coefficients showed that the standardized path coefficient between Tc and actual discharge was 0.242 ($p < 0.001$), whereas that between rated flow rate and actual discharge was 0.689 ($p < 0.001$). Tc and electricity consumption exhibited a significant negative path relationship ($\beta = -1.561$, $p < 0.001$). The path relationship between rated flow rate and irrigated area was significant ($\beta = 5.584$, $p = 0.026$), and rated flow rate was also significantly associated with aquifer water-yield potential ($\beta = 1.074$, $p < 0.001$). The path relationships of actual discharge and rated flow rate with groundwater depth had *p*-values of 0.097 and 0.099, respectively; neither reached the 0.05 significance level, and they were therefore described only as marginal associations. The paths associated with pump power and lithology were also not statistically significant.

All significance tests were assessed using Z statistics. Differences in effect sizes among key paths indicated complex interactions among the latent variables. Most fit indices, including the chi-square test *p*-value of 0.13, chi-square-to-degrees-of-freedom ratio of 1.23, GFI of 0.93, RMSEA of 0.06, RMR of 0.03, CFI of 0.93, NFI of 0.93, and NNFI of 0.92, met the criteria for good model fit, indicating that the SEM fitted the data well (Table 3).

Table 3. SEM model fit indices.

χ^2	df	*p*	GFI	RMSEA	RMR	CFI	NFI	NNFI
-	-	>0.05	>0.9	<0.10	<0.05	>0.9	>0.9	>0.9
6.54	14	0.13	0.93	0.06	0.03	0.93	0.93	0.92

3.4. Contributions of Environmental Variables to the Electricity-to-Water Conversion Coefficient

Redundancy analysis was conducted to examine the relationships of Tc, actual discharge, and electricity consumption with elevation, aquifer water-yield potential, well depth, groundwater depth, lithology, rated flow rate, pump power, well completion date, casing inside diameter, and irrigated area in Chayouzhongqi (Figure 5, left panel). The eigenvalues of Axis 1 and Axis 2 were 0.49 and 0.12, respectively. The selected environ-

mental variables collectively explained 60.53% of the variation in Tc. Tc, actual discharge, and electricity consumption showed different directions of association with well–pump operating variables and hydrogeological variables.

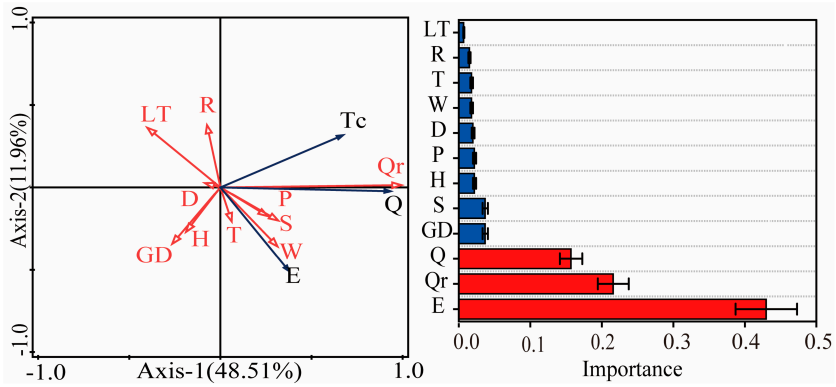

Figure 5. Redundancy analysis and variable-importance analysis of the electricity-to-water conversion coefficient and associated variables. Note: The **left** panel shows redundancy analysis (RDA), and the **right** panel shows variable-importance ranking from random forest (RF) analysis. Tc, electrici-ty-to-water conversion coefficient; Q, actual discharge; E, electricity consumption; Qr, rated flow rate; H, elevation; W, aquifer water-yield potential; D, well depth; GD, groundwater depth; LT, lithology; P, pump power; T, well completion date; R, casing inside diameter; and S, irrigated area.

Random forest analysis (Figure 5, right panel) indicated relative importance values of 43.0%, 21.6%, and 15.7% for electricity consumption, rated flow rate, and actual discharge, respectively. The random forest parameter settings are presented in Table 4.

Table 4. Random forest model parameters.

Parameter	Value	Description
Data-splitting ratio	70%/30%	Seventy percent of the data was used for training and 30% for testing.
Data shuffling	Yes	Reduced the influence of sample order on model training.
Cross-validation	Yes	Used to evaluate model stability.
Node-splitting criterion	MSE	Suitable for regression analysis with continuous Tc as the dependent variable.
Maximum number of features considered for splitting	sqrt	Increased model randomness and reduced the risk of overfitting.
Maximum tree depth	None	No maximum depth was specified; tree growth was controlled by node-splitting conditions.
Minimum samples required to split an internal node	5	Restricted excessively small node splits and reduced the risk of overfitting.
Minimum samples per leaf node	5	Improved model generalizability.
Minimum weighted fraction of samples in a leaf node	0	Default setting.
Minimum impurity decrease	1×10^{-7}	Avoided invalid or extremely weak splits.
Number of decision trees	205	Improved model stability.
Bootstrap sampling	TRUE	Decision trees were constructed using bootstrap sampling.
Out-of-bag data testing	TRUE	Used to assist the evaluation of model generalizability.

3.5. Differences in Tc Under Different Well–Pump Operating Conditions, Well-Depth Classes, and Aquifer Water-Yield Potential

To further describe Tc variation under different well–pump operating conditions and hydrogeological settings, Tc was grouped according to rated flow rate, pump power, well depth, and aquifer water-yield potential.

Across rated-flow-rate classes, actual discharge and Tc showed an overall positive relationship, although the degree of dispersion differed among flow-rate classes (Figure 6). Within the rated-flow-rate range of 20–40 m^3 h^{-1}, the observations were relatively concentrated, and the linear fitted relationship was comparatively stable. As the rated flow rate increased further, the dispersion of observations increased.

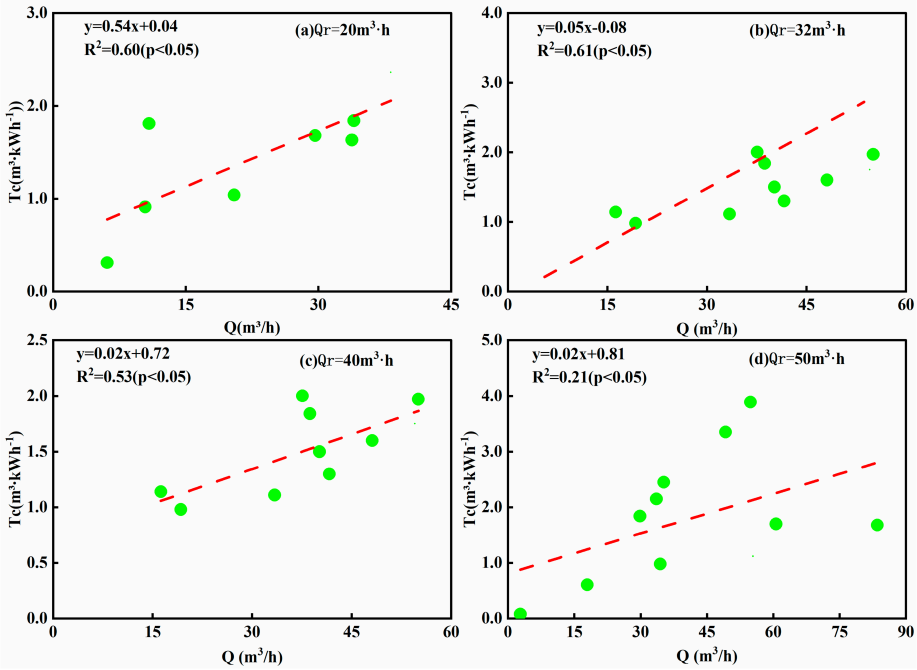

Figure 6. Relationship between actual discharge and the electricity-to-water conversion coefficient at different rated flow rates.

Across pump-power classes, both the mean Tc and its degree of dispersion differed to some extent (Table 5). The 18–25 kW range contained relatively more observations, and mean Tc values were comparatively stable. Low- and high-power pump groups showed wider Tc ranges because of their smaller sample sizes or greater differences in operating conditions.

Table 5. Tc statistics across pump-power classes.

Pump Power (kW)	Number of Data Points	Average m^3/(kW·h)	Maximum m^3/(kW·h)	Minimum m^3/(kW·h)	Standard Deviation
7.5	2	1.22	2.36	0.08	1.61
9.5	1	1.97	1.97	1.97	-
11.0	3	1.11	1.63	0.78	0.43
15.0	10	1.66	3.25	0.41	0.73
16.0	1	1.77	1.77	1.77	-
18.0	4	1.64	2.00	1.01	0.43
18.5	10	1.82	3.88	0.88	0.88
20.0	1	1.84	1.84	1.84	-
22.0	8	1.69	3.35	0.31	0.86

Table 5. *Cont.*

Pump Power (kW)	Number of Data Points	Average $m^3/(kW \cdot h)$	Maximum $m^3/(kW \cdot h)$	Minimum $m^3/(kW \cdot h)$	Standard Deviation
25.0	6	1.6	2.45	0.98	0.56
26.0	1	0.61	0.61	0.61	-
30.0	3	1.27	2.15	0.6	0.78
32.0	1	1.11	1.11	1.11	-
37	3	2.59	3.88	1.26	1.32

Tc also differed among well-depth classes (Figure 7). The 50–100 m and 100–150 m depth classes contained more observations and therefore better represented the Tc distribution under intermediate well-depth conditions in the study area. Tc values in the 150–200 m depth class were generally lower.

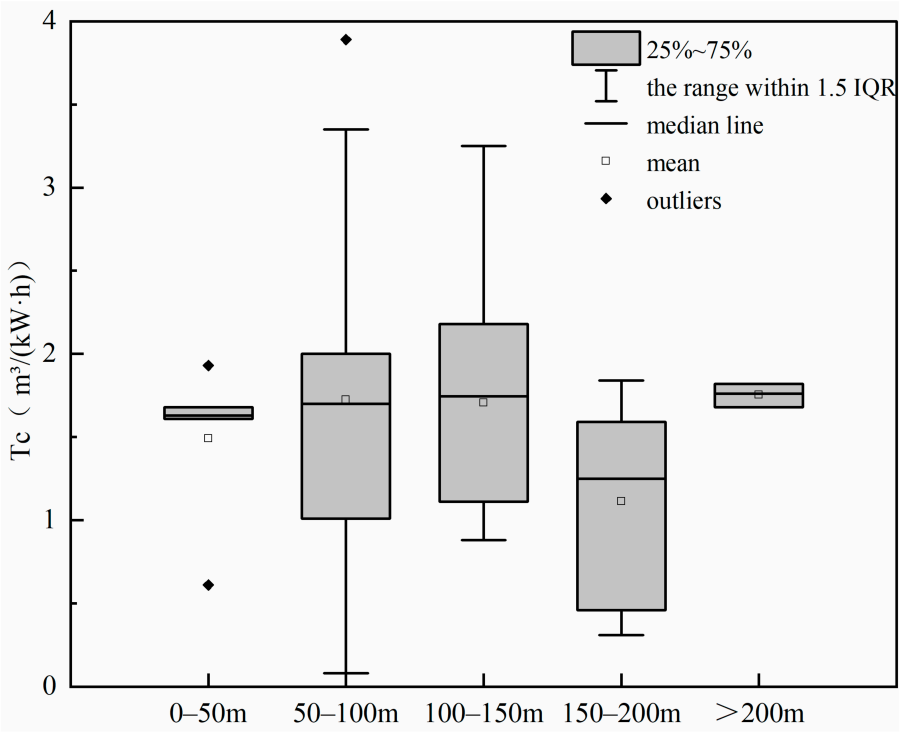

Figure 7. Distribution of the electricity-to-water conversion coefficient across well-depth classes. Note: The number of observations in the 0–50 m, 50–100 m, 100–150 m, 150–200 m, and >200 m well-depth classes were 4, 19, 22, 10, and 1, respectively, for a total of 56 observations.

The grouped results for groundwater type and aquifer water-yield potential showed differences in Tc among aquifer water-yield-potential classes (Table 6). In some areas with relatively high aquifer water-yield potential, Tc was also relatively high, suggesting that aquifer water-supply capacity may influence the well-discharge process. However, aquifer water-yield potential did not show a simple linear increasing relationship with Tc. This finding indicates that Tc is associated not only with aquifer water-yield potential but also with well depth, groundwater depth, rated flow rate, pump power, and actual operating conditions. Therefore, aquifer water-yield-potential results should be interpreted together with well–pump operating parameters rather than being simply summarized as "higher aquifer water-yield potential leads to higher Tc".

Table 6. Relationship between the electricity-to-water conversion coefficient, groundwater type, and aquifer water-yield potential.

Groundwater Type	Aquifer Water-Yield Potential (m^3/d)	Northern Irrigation District ($m^3/(kW·h)$)	Southern Irrigation District ($m^3/(kW·h)$)
Neogene clastic rocks Fractured and porous confined aquifer	>3000	1.05	—
	2000~3000	2.63	2.21
	1000~2000	1.46	1.47
	500~1000	2.31	1.99
	100~500	1.38	1.44
	<100	1.5	1.31
Neogene clastic rocks Fractured and porous unconfined aquifer	>1000	—	1.41
	500–1000	—	1.83
	<500	—	1.49
Neogene basalt Pore and fracture confined aquifer	>500	—	1.84
	<500	—	0.41
Quaternary loose rock Pore unconfined aquifer	500–1000	—	0.86

Note: Groundwater types and aquifer water-yield-potential classes were based on regional hydrogeological survey data from the Department of Water Resources of the Inner Mongolia Autonomous Region. The delineation of the northern and southern irrigation districts and the Tc statistics were based on the monitoring-well data collected in this study.

4. Discussion

4.1. Spatial Distribution Characteristics of the Electricity-to-Water Conversion Coefficient

The broad range of Tc variation in Chayouzhongqi reflects the high sensitivity of the water–energy–geology coupling process in water-resource development and utilization in arid and semi-arid regions. Under conditions of limited precipitation, intense evaporation, and restricted recharge, groundwater abstraction often requires greater pumping heads and more stable energy inputs, thereby amplifying the spatial variation in Tc [2,23]. The topography of the study area provides the macro-scale framework for this coupled system. Topographic variation not only directly controls pumping head and substantially affects electricity consumption [23,24], but also shapes aquifer structure and patterns of aquifer water-yield potential by regulating sedimentary environments and groundwater recharge–runoff–discharge conditions. These processes further result in marked spatial heterogeneity in groundwater depth and groundwater extractability [25,26].

Tc showed a spatial pattern of higher values in the north, lower values in the south, and the lowest values in the west. This pattern was closely related to the transition from the northern plains to the southern and western hilly and mountainous areas. In topographic transition zones, lower aquifer water-yield potential and greater groundwater depth may increase the difficulty of groundwater abstraction and pumping head, thereby reinforcing Tc differences through a chain effect of "greater groundwater depth–higher pumping head–greater electricity consumption–higher Tc" [27–29]. Overall, topographic factors are not only key external constraints for explaining the spatial differentiation of Tc at the regional scale, but also important indicators for improving the energy efficiency of motor-pumped wells and refining groundwater management in arid and semi-arid regions.

4.2. Factors Associated with Electricity-to-Water Conversion Coefficient

Tc is essentially a measure of the overall efficiency with which a pump unit converts electrical energy into hydraulic energy for water lifting [6]. Accordingly, Tc was positively associated with rated flow rate and actual discharge and negatively associated with electricity consumption, which is a basic characteristic of high-efficiency systems [6,7]. The

results indicate that electricity consumption, rated flow rate, and actual discharge are the main operating variables representing variation in Tc. It should be emphasized that electricity consumption and actual discharge are direct components of the Tc calculation. Their correlations with Tc are therefore partly influenced by the definition of the indicator itself and should not be interpreted simply as independent external driving factors [7,30–32].

Accordingly, electricity consumption, actual discharge, and rated flow rate were interpreted as direct indicators of well–pump operating conditions, whereas well depth, groundwater depth, aquifer water-yield potential, lithology, and elevation were interpreted as external topographic and hydrogeological constraints. In other words, regional topography and aquifer conditions do not necessarily alter Tc directly; rather, they may indirectly influence Tc by affecting pumping head, water-supply capacity, and well–pump operating conditions.

From the perspective of well–pump operation, higher actual discharge generally indicates stronger well water-supply capacity per unit time. Under the same or similar electricity-consumption conditions, increasing discharge increases the volume of water withdrawn per unit of electricity consumed. The rated flow rate reflects the design operating conditions of the pump and the configuration of the well system. Its relationship with Tc indicates that matching of pump parameters is important for the electricity-to-water conversion process [33]. However, substantial dispersion remained within rated-flow-rate groups, indicating that Tc is not determined solely by rated parameters. Actual pumping head, groundwater depth, pipeline losses, and aquifer recharge capacity may also affect operating efficiency [7,34]. Therefore, no specific flow rate was defined as a clear optimal operating threshold; instead, the increased dispersion in high-flow groups was interpreted as a statistical phenomenon under the combined influence of multiple factors.

The well-depth grouping results showed that Tc was generally lower in the 150–200 m depth class, suggesting that increasing well depth may reduce Actual discharge per unit of electricity by increasing pumping head and energy demand [35,36]. However, the 0–50 m and >200 m classes had small sample sizes, which contained only one observation. Therefore, the results cannot be used to infer a stable Tc rebound under deep-well conditions or to directly demonstrate the contribution of deep confined aquifers [35]. The differences among well-depth groups are discussed only as trends. Further verification will require more deep-well samples, borehole information, and long-term groundwater-level monitoring data.

The grouping results for aquifer water-yield potential further indicate that aquifer water-supply capacity imposes some constraint on Tc, although the relationship is not simply linear. Higher aquifer water-yield potential may improve well discharge capacity; however, Tc may still vary substantially when pump configuration, actual pumping head, or pipeline conditions are not appropriately matched. Therefore, Tc formation in plateau well-irrigation districts should be understood as the combined result of hydrogeological background, well–pump operating conditions, and electricity-to-water conversion efficiency. This finding also indicates that empirical coefficients developed for plain irrigation districts should not be directly applied to plateau areas with pronounced topographic relief and complex aquifer conditions; regional calibration is necessary [37,38].

4.3. Comparative Analysis with Other Regions in China and Abroad

Comparison of Chayouzhongqi with typical well-irrigation districts under different climatic zones and hydrogeological settings indicates that the electricity-to-water conversion coefficient (Tc) is fundamentally an integrated representation of the coupled effects of hydrogeological conditions, engineering equipment performance, and irrigation systems.

Its spatial differentiation patterns and associated mechanisms therefore exhibit both general commonalities and regional specificities.

Previous studies have shown that the energy performance of groundwater irrigation is not determined by a single factor. The volume of water withdrawn and total head, including groundwater lifting height, drawdown, and the pressure required by pipeline and irrigation systems, jointly determine theoretical energy consumption. Groundwater depth, pumping efficiency, aquifer conditions, and irrigation-system type may further contribute to differences in energy use [1,3,39,40]. Accordingly, groundwater-level decline or increased pumping head generally requires more energy per unit volume of water withdrawn; however, the magnitude of this change also depends on aquifer water-supply capacity, pump efficiency, well–pump matching, and irrigation method. Estimating groundwater abstraction from electricity consumption requires establishing a relationship between energy use and water withdrawal for the specific study area [41]. The applicability of different groundwater-abstraction estimation methods is also affected by data availability, spatial and temporal resolution, and estimation accuracy [42]. Therefore, under complex topographic and hydrogeological conditions, fixed coefficients from other regions should not be applied unconditionally; regional calibration is more appropriate.

This study was based on a single-period survey of 56 typical wells, and the regional calibration model primarily reflects within-sample relationships under typical well-irrigation conditions in Chayouzhongqi. Its extrapolative applicability requires validation using independent data from other regions and multiple seasons. In this study, electricity consumption, rated flow rate, and actual discharge ranked highly in the variable-importance analysis, whereas well depth, groundwater depth, and aquifer water-yield potential represented external background constraints. This pattern is consistent with previous findings that hydrogeological conditions influence well water-supply capacity and pumping head, whereas well–pump and irrigation systems determine the energy-conversion process [1,3,39,42].

5. Conclusions

(1) In Chayouzhongqi, Tc ranged from 0.08 to 3.88 m^3 kWh^{-1}, with an arithmetic mean of 1.62 m^3 kWh^{-1}, indicating substantial differences in groundwater abstraction per unit of electricity consumed across the study area. Tc was generally higher in the north, lower in the south, and lowest in the west, indicating pronounced spatial heterogeneity in plateau well-irrigation districts.

(2) Electricity consumption, rated flow rate, and actual discharge were the main well–pump operating variables representing variation in Tc, with relative importance values of 43.0%, 21.6%, and 15.7%, respectively. Electricity consumption and actual discharge are direct components of the Tc calculation. In contrast, well depth, groundwater depth, aquifer water-yield potential, lithology, and elevation mainly impose indirect constraints on Tc by affecting pumping head, aquifer water-supply capacity, and well–pump matching conditions.

(3) The main variation patterns of the electricity-to-water conversion coefficient (Tc) under typical well-irrigation conditions in Chayouzhongqi indicate that Tc in plateau well-irrigation districts should not directly adopt empirical values from plain irrigation districts, but should instead be specifically calibrated according to local hydrogeological conditions and well–pump operating characteristics.

6. Limitations and Future Perspectives

This study has several limitations. Although the 56 typical wells covered the main landform units, well-depth classes, pump-power types, and irrigation methods in Chayouzhongqi, the sample size remains limited relative to the total number of motor-pumped

wells in the region. Therefore, the present results are more appropriate for identifying spatial differences in Tc and the major associated factors within typical well-irrigation systems in the study area, rather than for well-by-well prediction across all irrigation wells. In addition, the data were collected only in July 2023 and primarily reflect spatial differences in Tc among wells during the survey period; they cannot yet reveal its seasonal or interannual variation. In arid and semi-arid regions, groundwater depth may vary with precipitation, evaporation, irrigation intensity, and groundwater recharge processes, thereby affecting pumping head, electricity consumption, and actual discharge. Consequently, the sensitivity of the regional calibration model to future groundwater-level changes and different hydrological conditions requires further evaluation.

Future research should be strengthened in four respects. First, the number of samples should be increased across different landform zones and well-depth classes, particularly for deep wells, to improve model applicability under extreme well-depth conditions and complex aquifer settings. Second, multi-season and multi-year continuous monitoring should be conducted to assess the effects of groundwater-level dynamics, irrigation regimes, and hydroclimatic conditions on Tc. Third, pump-performance curves, actual pumping head, pipeline losses, and well-specific aquifer parameters should be incorporated to develop a more comprehensive Tc estimation model. Finally, independent validation should be conducted in other plateau or arid and semi-arid well-irrigation districts to evaluate the transferability and applicability boundaries of the regional calibration model.

Author Contributions: H.Z.: formal analysis, methodology, software, writing—original draft preparation. B.G.: formal analysis, methodology, software, writing—original draft preparation (equal contribution). X.S.: data curation, funding acquisition, methodology, resources, supervision. J.L.: conceptualization, methodology, supervision. Y.L.: project administration, supervision, data curation, writing—review and editing. W.L.: conceptualization, supervision. L.X.: conceptualization, supervision. All authors have read and agreed to the published version of the manuscript.

Funding: The research was supported by the 2025 Science and Technology Support Project of the State Key Laboratory of Water Engineering Ecology and Environment in Arid Area (2025GJCXPT01018), the National Natural Science Foundation of China (projects U2443225, 52260028, 52369014, and 52260029), the Inner Mongolia Autonomous Region Education Special Fund (2025), the Inner Mongolia Autonomous Region Science and Technology Plan (projects 2025KYPT0099, 2023YFDZ0022, 2025LHMS04019, and 2025YFHH0188), the Basic Research Funds for Higher Education Institutions in the Inner Mongolia Autonomous Region (BR251202, BR251009, and BR230402), the Inner Mongolia Association for Science and Technology Young Scientist Support Project for Doctoral Students (QTBS2526), and the Inner Mongolia Autonomous Region Leading Talent Team project (2022LJRC0007).

Data Availability Statement: The original contributions presented in this study are included in the article. Further inquiries can be directed to the corresponding author.

Conflicts of Interest: The authors declare no conflicts of interest.

References

1. Shayanmehr, S.; Porhajašová, J.I.; Babošová, M.; Sabouhi Sabouni, M.; Mohammadi, H.; Rastegari Henneberry, S.; Shahnoushi Foroushani, N. The Impacts of Climate Change on Water Resources and Crop Production in an Arid Region. *Agriculture* **2022**, *12*, 1056. [CrossRef]
2. Aeschbach-Hertig, W.; Gleeson, T. Regional strategies for the accelerating global problem of groundwater depletion. *Nat. Geosci.* **2012**, *5*, 853–861. [CrossRef]
3. Siyal, A.W.; Gerbens-Leenes, P.W.; Nonhebel, S. Energy and carbon footprints for irrigation water in the lower Indus basin in Pakistan, comparing water supply by gravity fed canal networks and groundwater pumping. *J. Clean. Prod.* **2021**, *286*, 125489. [CrossRef]

4. Chu, H.J.; Lin, C.W.; Burbey, T.J.; Ali, M.Z. Spatiotemporal Analysis of Extracted Groundwater Volumes Estimated from Electricity Consumption. *Groundwater* **2020**, *58*, 962–972. [CrossRef] [PubMed]
5. Salman, A.K.; Alhadeethi, I.K.; Mohammed, A.M.; Sut-Lohmann, M. Assessing irrigation system efficiency within the Water-Energy-Food Nexus: Introducing energy performance metrics. *Agric. Water Manag.* **2025**, *317*, 109665. [CrossRef]
6. Koushki, R.; Warren, J.; Krzmarzick, M.J. Carbon footprint of agricultural groundwater pumping with energy demand and supply management analysis. *Irrig. Sci.* **2024**, *42*, 735–744. [CrossRef]
7. Loureiro, D.; Beceiro, P.; Fernandes, E.; Alegre, H.; Covas, D. Energy efficiency assessment in collective irrigation systems using water and energy balances: Methodology and application. *Irrig. Sci.* **2024**, *42*, 745–768. [CrossRef]
8. Chen, X.; Thorp, K.R.; Ouyang, Z.; Hou, Y.; Zhou, B.; Li, Y. Energy consumption due to groundwater pumping for irrigation in the North China Plain. *Sci. Total Environ.* **2019**, *669*, 1033–1042. [CrossRef] [PubMed]
9. Ke, H.; Zhang, F.; Sikai, Y.; Zhe, M.; Bin, X. Using Machine Learning Models to Forecast the Conversion Coefficient between Electricity Consumption and Water Pumped for Irrigation Wells in Baicheng City, China. *Water* **2024**, *16*, 523. [CrossRef]
10. Chahar Right Middle Banner People's Government. Natural Overview of Chahar Right Middle Banner. Available online: https://www.cyzq.gov.cn/zrgk/index.html (accessed on 19 May 2026).
11. Zhao, G. Study on Water Resources and Water-Saving Agricultural Technologies in Chayouzhongqi, Inner Mongolia. Master's Thesis, Chinese Academy of Agricultural Sciences, Beijing, China, 2006.
12. Ba, T.; Xu, G.M.; Fu, Z.Q.; Zhang, F.Y.; Tian, X.L. Climatic Condition Analysis and Division of Potato Planting in Chayouzhong County. *Meteorol. J. Inn. Mong.* **2009**, *4*, 30–32. (In Chinese)
13. Ma, W. Protection and Governance of the Mining Geological Environment of the Yinggong Mountain Granite Mine in Chayouzhongqi, Inner Mongolia. Master's Thesis, China University of Geosciences, Beijing, China, 2016.
14. Chen, X.; Zhang, G.; Jin, Y.; Mao, S.; Laakso, K.; Sanchez-Azofeifa, A.; Jiang, L.; Zhou, Y.; Zhao, H.; Yu, L.; et al. Evaluating the farmland use intensity and its patterns in a farming–pastoral ecotone of northern China. *Remote Sens.* **2021**, *13*, 4304. [CrossRef]
15. Li, F.; Tao, P.; Qi, Y.Q.; Li, H.J.; Wang, H.X.; Wang, N.; Pei, H.W.; Zhang, X.Y. Factors influencing electricity-to-water conversion metering method for irrigation water consumption in Hebei Plain. *Chin. J. Eco-Agric.* **2022**, *30*, 1993–2001. [CrossRef]
16. Wang, L.; Kinzelbach, W.; Yao, H.; Steiner, J.; Wang, H. How to Meter Agricultural Pumping at Numerous Small-Scale Wells?—An Indirect Monitoring Method Using Electric Energy as Proxy. *Water* **2020**, *12*, 2477. [CrossRef]
17. Hill, C.J.; Moore, T.; Dumville, M. Carrier Phase Surveying with Garmin Handheld GPS Receivers. *Surv. Rev.* **2001**, *36*, 135–141. [CrossRef]
18. Rashed, M. Dual-function water-level/well-depth meter. *Measurement* **2020**, *152*, 107326. [CrossRef]
19. Zhang, H.; Shi, X.; Zhao, S.; Quan, D.; Sun, B.; Zhang, S. Eutrophication Characteristics and Influencing Factors of the Eastern Lake of Chagannaoer Lake Inner Mongolia. *Wetl. Sci.* **2023**, *21*, 842–849.
20. Zhao, Y.; Wang, Q.; Jiang, S.; Zhai, J.; Wang, J.; He, G.; Li, H.; Zhang, Y.; Wang, L.; Zhu, Y. Irrigation water and energy saving in well irrigation district from a water-energy nexus perspective. *J. Clean. Prod.* **2020**, *267*, 122058. [CrossRef]
21. Fan, Y.; Chen, J.; Shirkey, G.; John, R.; Wu, S.R.; Park, H.; Shao, C. Applications of structural equation modeling (SEM) in ecological studies: An updated review. *Ecol. Process* **2016**, *5*, 19. [CrossRef]
22. Wollenberg, A.L. Redundancy Analysis an Alternative for Canonical Correlation Analysis. *Psychometrika* **1977**, *42*, 207–219. [CrossRef]
23. Qin, J.; Duan, W.; Zou, S.; Chen, Y.; Huang, W.; Rosa, L. Global energy use and carbon emissions from irrigated agriculture. *Nat. Commun.* **2024**, *15*, 3084. [CrossRef] [PubMed]
24. Okakwu, I.K.; Alayande, A.S.; Akinyele, D.O.; Olabode, O.E.; Akinyemi, J.O. Effects of total system head and solar radiation on the techno-economics of PV groundwater pumping irrigation system for sustainable agricultural production. *Sci. Afr.* **2022**, *16*, e01118. [CrossRef]
25. Tóth, J. A theoretical analysis of groundwater flow in small drainage basins. *J. Geophys. Res.* **1963**, *68*, 4795–4812. [CrossRef]
26. Xiao, Y.; Shao, J.; Frape, S.K.; Cui, Y.; Dang, X.; Wang, S.; Ji, Y. Groundwater Origin, Flow Regime and Geochemical Evolution in Arid Endorheic Watersheds: A Case Study from the Qaidam Basin, Northwestern China. *Hydrol. Earth Syst. Sci.* **2018**, *22*, 4381–4400. [CrossRef]
27. Hossain, M.S.; Chowdhury, M.M.; Das, B.K.; Islam, M.R.; Kibria, M.G.; Banik, S. A sustainable energy approach for pumping and irrigation in the Barind Region of Bangladesh. *Clean Technol. Environ. Policy* **2024**, *26*, 2151–2180. [CrossRef]
28. Scanlon, B.R.; Faunt, C.C.; Longuevergne, L.; Reedy, R.C.; Alley, W.M.; McGuire, V.L.; McMahon, P.B. Groundwater depletion and sustainability of irrigation in the US High Plains and Central Valley. *Proc. Natl. Acad. Sci. USA* **2012**, *109*, 9320–9325. [CrossRef] [PubMed]
29. Stringer, L.C.; Mirzabaev, A.; Benjaminsen, T.A.; Harris, R.M.B.; Jafari, M.; Lissner, T.K.; Stevens, N.; Tirado-von der Pahlen, C. Climate change impacts on water security in global drylands. *One Earth* **2021**, *4*, 851–864. [CrossRef]
30. Breiman, L. Random Forests. *Mach. Learn.* **2001**, *45*, 5–32. [CrossRef]

31. Kronmal, R.A. Spurious Correlation and the Fallacy of the Ratio Standard Revisited. *J. R. Stat. Soc. Ser. A (Stat. Soc.)* **1993**, *156*, 379. [CrossRef]
32. Brett, M.T. When is a correlation between non-independent variables "spurious"? *Oikos* **2004**, *105*, 647–656. [CrossRef]
33. Cui, S.; Wu, M.; Huang, X.; Cao, X. Unravelling resources use efficiency and its drivers for water transfer and grain production processes in pumping irrigation system. *Sci. Total Environ.* **2022**, *818*, 151810. [CrossRef] [PubMed]
34. Helweg, O.J. Economics of Improving Well and Pump Efficiency. *Groundwater* **1982**, *20*, 556–562. [CrossRef]
35. Gao, X.; Liu, J.; Zhang, J.; Yan, J.; Bao, S.; Xu, H.; Qin, T. Feasibility evaluation of solar photovoltaic pumping irrigation system based on analysis of dynamic variation of groundwater table. *Appl. Energy* **2013**, *105*, 182–193. [CrossRef]
36. Driscoll, A.W.; Conant, R.T.; Marston, L.T.; Choi, E.; Mueller, N.D. Greenhouse gas emissions from US irrigation pumping and implications for climate-smart irrigation policy. *Nat. Commun.* **2024**, *15*, 675. [CrossRef] [PubMed]
37. Mekonnen, D.; Siddiqi, A.; Ringler, C. Drivers of groundwater use and technical efficiency of groundwater, canal water, and conjunctive use in Pakistan's Indus Basin Irrigation System. *Int. J. Water Resour. Dev.* **2016**, *32*, 459–476. [CrossRef]
38. Rubio-Aliaga, Á.; García-Cascales, M.S.; Sánchez-Lozano, J.M.; Molina-García, A. Multidimensional analysis of groundwater pumping for irrigation purposes: Economic, energy and environmental characterization for PV power plant integration. *Renew. Energy* **2019**, *138*, 174–186. [CrossRef]
39. Shandilya, R.N.; Bresciani, E.; Kang, P.K.; Lee, S. Influence of hydrogeological and operational parameters on well pumping capacity. *J. Hydrol.* **2022**, *608*, 127643. [CrossRef]
40. Alam, M.F.; Pavelic, P.; Sikka, A.; Krishnan, S.; Dodiya, M.; Bhadaliya, P.; Joshi, V. Energy consumption as a proxy to estimate groundwater abstraction in irrigation. *Groundw. Sustain. Dev.* **2023**, *23*, 101035. [CrossRef]
41. Brookfield, A.E.; Zipper, S.; Kendall, A.D.; Ajami, H.; Deines, J.M. Estimating Groundwater Pumping for Irrigation: A Method Comparison. *Groundwater* **2024**, *62*, 15–33. [CrossRef] [PubMed]
42. Benson, D.A.; Miller, S.; Barber, J. Markov-chain Monte Carlo estimation of aquifer parameters, non-linear well losses, and probable costs of water extraction. *J. Hydrol.* **2026**, *668*, 134952. [CrossRef]

Disclaimer/Publisher's Note: The statements, opinions and data contained in all publications are solely those of the individual author(s) and contributor(s) and not of MDPI and/or the editor(s). MDPI and/or the editor(s) disclaim responsibility for any injury to people or property resulting from any ideas, methods, instructions or products referred to in the content.